

Jiří Homola

## Present and future of surface plasmon resonance biosensors

Received: 20 March 2003 / Revised: 4 June 2003 / Accepted: 5 June 2003 / Published online: 19 July 2003

© Springer-Verlag 2003

**Abstract** Surface plasmon resonance (SPR) biosensors are optical sensors exploiting special electromagnetic waves – surface plasmon-polaritons – to probe interactions between an analyte in solution and a biomolecular recognition element immobilized on the SPR sensor surface. Major application areas include detection of biological analytes and analysis of biomolecular interactions where SPR biosensors provide benefits of label-free real-time analytical technology. This paper reviews fundamentals of SPR affinity biosensors and discusses recent advances in development and applications of SPR biosensors.

**Keywords** Optical sensor · Biosensor · Affinity biosensor · Immunosensor · Surface plasmon resonance

### Introduction

The last two decades have witnessed remarkable progress in the development of affinity biosensors and their applications in areas such as environmental protection, biotechnology, medical diagnostics, drug screening, food safety, and security. An affinity biosensor consists of a transducer (electrochemical [1], piezoelectric [2], or optical [3]) and a biological recognition element which is able to interact with a selected analyte. Various optical methods have been exploited in biosensors including fluorescence spectroscopy [4], interferometry (reflectometric white light interferometry [5] and modal interferometry in optical waveguide structures [6]), spectroscopy of guided modes of optical waveguides (grating coupler [7] and resonant mirror [8]), and surface plasmon resonance (SPR) [9, 10]. Fluorescence-based biosensors offer high sensitivity but, due to the use of labels, they require either multi-step de-

tection protocols or delicately balanced affinities of interacting biomolecules for displacement assays, causing sensor cross-sensitivity to non-target analytes [11]. Sensors such as optical interferometers, grating coupler, resonant mirror, and SPR rely on the measurement of binding-induced refractive index changes and thus are label-free technologies. This paper focuses on SPR biosensor technology, reviews fundamentals of SPR sensing, and discusses advances in development and applications of SPR biosensors and emerging trends in SPR biosensing.

### Fundamentals of surface plasmon resonance (SPR) biosensors

Surface plasmon-polariton

A surface plasma wave (SPW) or a surface plasmon-polariton is an electromagnetic wave which propagates along the boundary between a dielectric and a metal, which behaves like quasi-free electron plasma [12, 13]. An SPW is a transverse-magnetic (TM) wave (magnetic vector is parallel to the plane of interface) and is characterized by the propagation constant and electromagnetic field distribution. The propagation constant of an SPW,  $\beta$ , can be expressed as:

$$\beta = \frac{\omega}{c} \sqrt{\frac{\epsilon_M \epsilon_D}{\epsilon_M + \epsilon_D}} \quad (1)$$

where  $\omega$  is the angular frequency,  $c$  is the speed of light in vacuum, and  $\epsilon_D$  and  $\epsilon_M$  are dielectric functions of the dielectric and metal, respectively [12, 13]. This equation describes an SPW if the real part of  $\epsilon_M$  is negative and its absolute value is smaller than  $\epsilon_D$ . At optical wavelengths this condition is fulfilled for several metals of which gold is most commonly employed in SPR biosensors. The real and imaginary parts of the propagation constant describe spatial periodicity and attenuation of an SPW in the direction of propagation, respectively [12]. The electromagnetic field of an SPW is confined at the metal–dielectric boundary and decreases exponentially into both media,

J. Homola (✉)  
Institute of Radio Engineering and Electronics,  
Academy of Sciences of the Czech Republic,  
Chaberská 57, Prague, Czech Republic  
e-mail: homola@ure.cas.cz

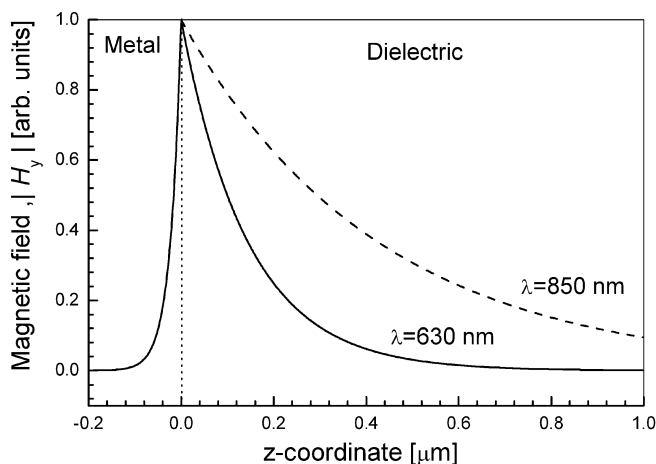


**Fig. 1** Distribution of the magnetic field intensity for an SPW at the interface between gold and dielectric (refractive index of the dielectric 1.32) in the direction perpendicular to the interface calculated for two different wavelengths

Fig. 1. For an SPW at the boundary between gold and a dielectric with a refractive index of 1.32 the penetration depth (the distance from the interface at which the amplitude of the field falls to  $1/e$  of its value at the metal surface) into the dielectric is typically 100–500 nm in the visible and near infrared regions [10, 13].

#### Concept of surface plasmon resonance biosensing

Owing to the fact that the vast majority of the field of an SPW is concentrated in the dielectric, the propagation constant of the SPW is extremely sensitive to changes in the refractive index of the dielectric. This property of SPW is the underlying physical principle of affinity SPR biosensors – biomolecular recognition elements on the surface of metal recognize and capture analyte present in a liquid sample producing a local increase in the refractive index at the metal surface. The refractive index increase gives rise to an increase in the propagation constant of SPW propagating along the metal surface (Fig. 2) which can be accurately measured by optical means.

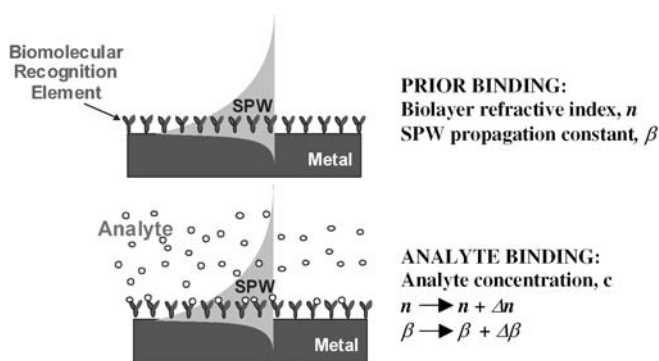


**Fig. 2** Principle of SPR biosensing

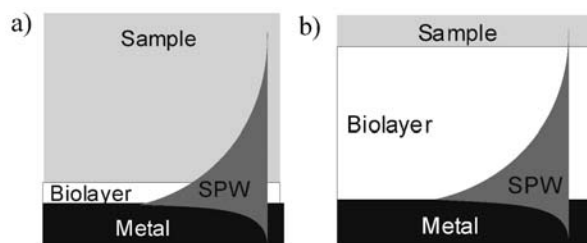


**Fig. 3** Surface plasmon-polariton probing: (a) biomolecular interaction occurring within a short distance from metal surface, and (b) biomolecular interaction occurring within the whole extent of the field of a SPW

The magnitude of the change in the propagation constant of an SPW depends on the refractive index change and its distribution with respect to the profile of the SPW field. There are two limiting cases:

1. analyte capture occurs only within a short distance from the metal surface (Fig. 3a), and
2. analyte capture occurs within the whole extent of the SPW field (Fig. 3b).

Perturbation theory [14] suggests that if the binding occurs within the whole depth of the SPW field (Fig. 3b), the binding-induced refractive index change,  $\Delta n$ , produces a change in the real part of the propagation constant,  $\Delta\beta$ , which is directly proportional to the refractive index change:

$$\text{Re}\{\Delta\beta\} \cong k\Delta n \quad (2)$$

where  $k$  denotes the free-space wavenumber [15]. If the refractive index change is caused by a binding event occurring within a distance from the surface  $d$ , much smaller than the penetration depth of the SPW, the corresponding change in the real part of the propagation constant can be expressed as follows:

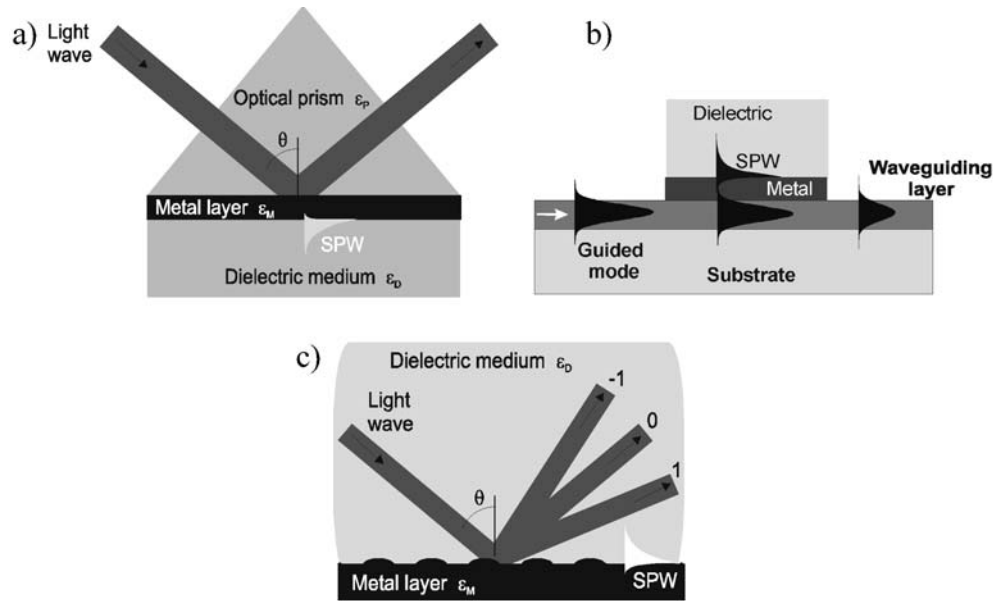
$$\text{Re}\{\Delta\beta\} \cong \frac{2n_s n_f k^2 d}{\sqrt{\text{Re}\{\epsilon_m\}}} \Delta n = Fk\Delta n \quad (3)$$

where  $n_f$  and  $n_s$  denote the refractive index of the biolayer and the refractive index of the background dielectric medium (sample), respectively. The binding-induced change in the propagation constant of the SPW is proportional to the refractive index change and the depth of the area within which the change occurs. The factor  $F$  ( $F < 1$ ) accounts for the fact that the interaction occurring within a thin layer is probed by only a fraction of the field of the SPW.

#### Excitation and interrogation of surface plasmon-polaritons

In SPR sensors, an SPW is excited by a light wave and the effect of this interaction on the characteristics of the light wave is measured. From these measurements, changes in the propagation constant of the SPW can be determined. Excitation of an SPW by light can occur only if the com-

**Fig. 4** Excitation of surface plasmon-polaritons: (a) by a light beam via prism coupling, (b) by a guided mode of optical waveguide, and (c) by light diffraction on a diffraction grating



ponent of the light's wave vector that is parallel to the metal surface matches that of the SPW. This can be achieved by means of prism coupling, waveguide coupling, and grating coupling.

In configurations based on prism coupling a light wave passes through a high refractive index prism and is totally reflected at the prism–metal layer interface generating an evanescent wave penetrating the metal layer (Fig. 4a). This evanescent wave propagates along the interface with a propagation constant which can be adjusted to match that of the SPW by controlling the angle of incidence. This method is referred to as the attenuated total reflection (ATR) method [13]. The process of exciting an SPW in an optical waveguide-based SPR structure (Fig. 4b) is similar to that in the ATR coupler. The light wave is guided by an optical waveguide and, when entering the region with a thin metal layer, it evanescently penetrates through the metal layer exciting an SPW at its outer boundary. Alternatively, an SPW can be excited by diffraction on a grating, Fig. 4c. The component of the wave vector of the diffracted waves parallel to the interface is diffraction-increased by an amount which is inversely proportional to the period of the grating and can be matched to that of an SPW [16]. The interaction of a light wave with an SPW can alter light's characteristics such as amplitude, phase, polarization and spectral distribution. Changes in these characteristics can be correlated with changes in the propagation constant of the SPW. Therefore, binding-induced changes in the refractive index at the sensor surface and, consequently, the propagation constant of the SPW can be determined by measuring changes in one of these characteristics. Based on which characteristic is measured, SPR biosensors can be classified as angle, wavelength, intensity, phase, or polarization modulation-based sensors. In SPR sensors with angular modulation the component of the light wave's wavevector parallel to the metal surface matching that of the SPW is determined by measuring the coupling strength at a fixed wavelength and multiple angles of incidence of the light wave and determining the angle of incidence

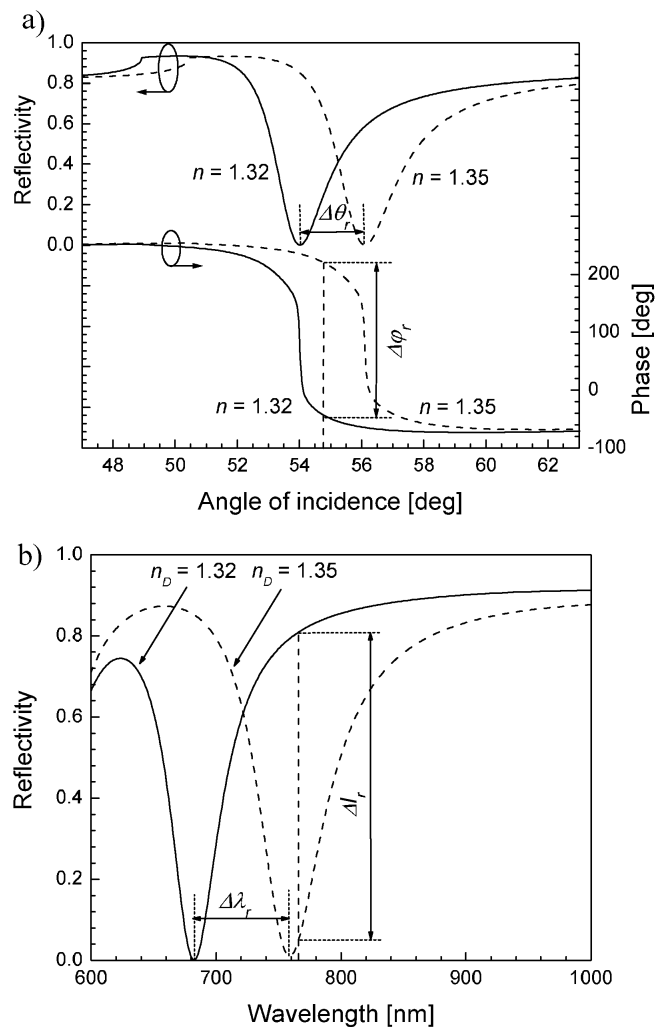


**Fig. 5** Reflectivity and phase for light wave exciting an SPW in the Kretschmann geometry (SF14 glass prism – 50 nm thick gold layer – dielectric) versus (a) the angle of incidence for two different refractive indices of the dielectric (wavelength 682 nm), and (b) wavelength for two different refractive indices of the dielectric (angle of incidence 54°)

yielding the strongest coupling (Fig. 5a, upper plot). In SPR sensors with wavelength modulation the component of the light wave's wavevector parallel to the metal surface matching that of the SPW is determined by measuring the coupling strength at a fixed angle of incidence and multiple wavelengths and determining the wavelength yielding the strongest coupling (Fig. 5b). In SPR sensors with intensity modulation, the change in the intensity of the light wave interacting with the SPW is measured at a fixed wavelength and angle of incidence (Fig. 5b). In SPR sensors with phase modulation, shift in phase of the light wave interacting with the SPW is measured at a fixed wavelength and angle of incidence (Fig. 5a, lower plot). In SPR sensors with polarization modulation, changes in the polarization are measured at a fixed wavelength and angle of incidence.

### Performance characteristics

The main performance characteristics relevant for SPR biosensors include sensitivity, accuracy, precision, repeatability, and the lowest detection limit. Sensor *sensitivity*  $S$ , is the ratio of the change in sensor output,  $P$  (e.g. angle of incidence, wavelength, intensity, phase, and polarization of light wave interacting with an SPW) to the change in measurand (e.g. analyte concentration,  $c$ ). SPR biosensor sensitivity can be decomposed into two components – sensitivity to refractive index changes produced by the binding of analyte to biomolecular recognition elements on the sensor surface  $S_{RI}$ , and the efficiency  $E$ , with which the presence of analyte at a concentration  $c$  is converted into the change in the refractive index  $n$ :

$$S = \frac{\partial P}{\partial n} \frac{\partial n}{\partial c} = S_{RI} E \quad (4)$$

The efficiency  $E$  depends on the properties of the biomolecular recognition elements and the target analyte. The refractive index sensitivity  $S_{RI}$  can be decomposed into two terms:

$$S_{RI} = \frac{\partial P}{\partial \text{Re}\{\beta\}} \frac{\partial \text{Re}\{\beta\}}{\partial n} = S_1 S_2 \quad (5)$$

The first term  $S_1$  depends on the modulation method and the method of excitation of an SPW [17, 18, 19, 20]. The  $S_2$  term is independent of the modulation method and the method of excitation of the SPW and describes the sensitivity of SPW's propagation constant to the refractive index change, Eqs. (2) and (3).

*Accuracy* describes the degree to which a sensor output represents the true value of the measurand (analyte concentration). Accuracy is often confused with *precision* which refers to the way in which repeated measurements conform to themselves without a reference to any true value. *Repeatability* refers to the capacity of a sensor to reproduce output reading under the same measurement conditions over a short interval of time. The *lowest detection limit* describes the lowest concentration of analyte that can be measured by the sensor.

### SPR biosensing formats

An interaction between a biomolecular recognition element on an SPR sensor surface and analyte in a liquid sample is governed by kinetic equations. In order to illustrate fundamental properties of the interaction, we shall discuss the pseudo-first-order kinetic equation:

$$\frac{dR}{dt} = k_a c (1 - R) - k_d R \quad (6)$$

where  $R$  is the relative amount of bound analyte,  $c$  is analyte concentration,  $t$  is time, and  $k_a$  and  $k_d$  are the association and dissociation kinetic rate constants, respectively [21]. This interaction model assumes 1:1 binding, rapid mixing of the analyte from the bulk phase to the sensor surface layer, and single-step binding. Observed binding, however, may deviate from this simple model due to more complex mechanisms of interaction and mass transport limitations [22]. Equation (6) yields for  $R$ :

$$R(t) = \left[ \frac{k_a c}{k_a c + k_d} - R_0 \right] \left( 1 - e^{-(k_a c + k_d)t} \right) + R_0 \quad (7)$$

where  $R_0$  denotes the initial amount of analyte bound at the time  $t=0$  [21].

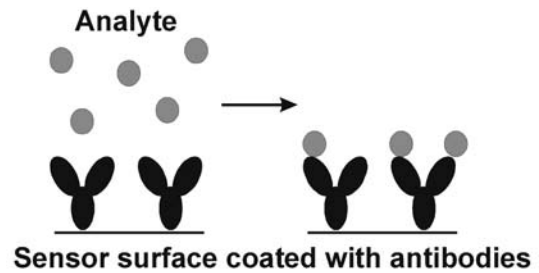


Fig. 6 Direct detection

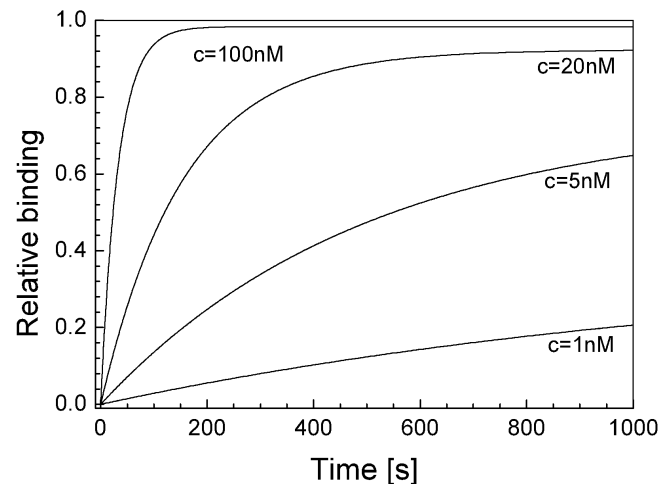
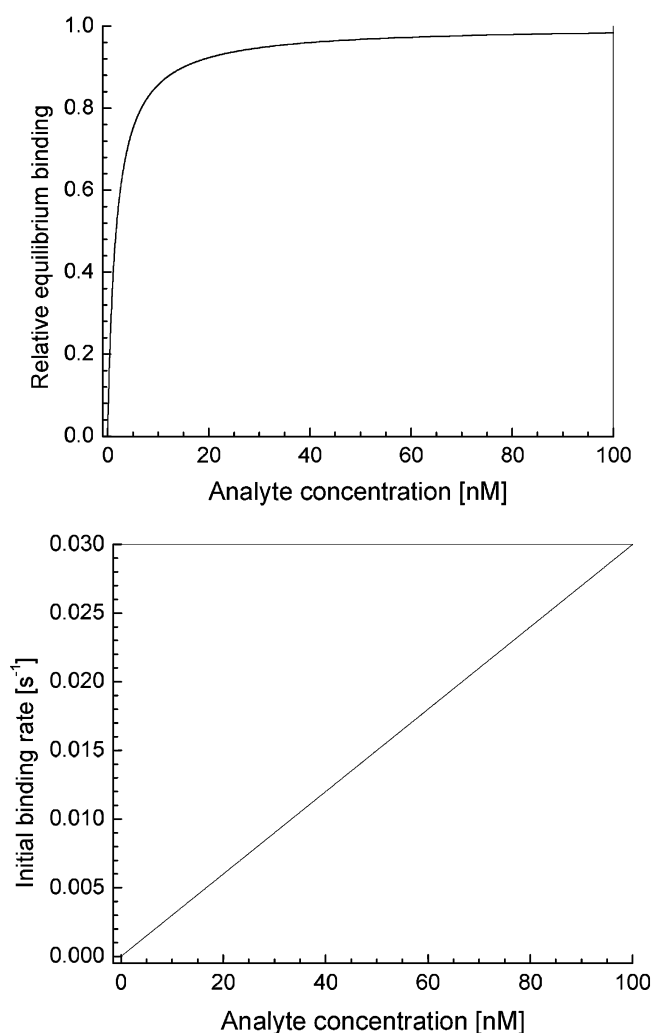


Fig. 7 Direct detection. Binding between antibody and analyte calculated for four different concentrations of analyte,  $k_a=3 \times 10^5 \text{ mol}^{-1} \text{ L s}^{-1}$ ;  $k_d=5 \times 10^{-4} \text{ s}^{-1}$

Various measurement formats have been adopted in SPR biosensing to ensure that the monitored binding event produces a measurable sensor response. The most frequently used measurement formats are direct detection, sandwich assay, and inhibition assay. In direct detection format, analyte in a sample interacts with a biomolecular recognition element (antibody) immobilized on the sensor surface, Fig. 6. The resulting refractive index change is directly proportional to the concentration of analyte.

Figure 7 which shows a kinetic model of the interaction between antibody and analyte suggests that the binding between the target analyte and antibody is fast initially. As the interaction progresses, the binding rate gradually decreases and eventually reaches a state in which the association and dissociation processes are in equilibrium. The time required for the interaction to reach the equilibrium depends on the concentration of analyte and is longer for lower concentrations of analyte.

Figure 8a shows dependence of the relative binding at equilibrium on the concentrations of analyte. At low ana-



**Fig. 8** Direct detection: (*top*) relative equilibrium binding as a function of analyte concentration; (*bottom*) initial binding rate as a function of analyte concentration,  $k_a=3\times 10^5 \text{ mol}^{-1} \text{ L s}^{-1}$ ;  $k_d=5\times 10^{-4} \text{ s}^{-1}$

lyte concentrations the equilibrium binding increases linearly with analyte concentration. At higher analyte concentrations, the binding sites provided by the biomolecular recognition elements are saturated and a further increase in the analyte concentration produces a smaller increase in the amount of bound analyte. The initial binding rate  $dR/dt$  ( $t=0$ ) is directly proportional to the association rate constant and analyte concentration (Fig. 8b). Both the amount of analyte bound at equilibrium and initial binding rate can be used to determine analyte concentration. The measurement of the binding rate is faster and offers a larger dynamic range than measurement of the equilibrium binding. In the *sandwich assay format* the measurement consists of two steps. In the first step, sample containing analyte is brought in contact with the sensor and the analyte molecules bind to the antibodies on the sensor surface. Then the sensor surface is incubated with a solution containing „secondary“ antibodies. The secondary antibodies bind to the previously captured analyte further increasing the number of bound biomolecules (Fig. 9) and thus also the sensor response.

The *inhibition assay* is an example of a competitive assay. In this detection format, a sample is initially mixed with respective antibodies and then the mixture is brought in contact with the sensor surface coated with analyte molecules, so that the unoccupied antibodies could bind to the analyte molecules (Fig. 10).

The amount of bound analyte versus time may be estimated by calculating the equilibrium concentration of antibody which did not bind to the analyte in the sample and then simulating the interaction between the unbound antibody and the analyte-derivatized surface. Figure 11 shows the equilibrium binding and the initial binding rate as a function of analyte concentration, assuming that antibody at a concentration of  $0.1 \text{ nmol L}^{-1}$  was incubated with sample and the mixture was provided with enough time to reach equilibrium. The amount of bound antibody and the

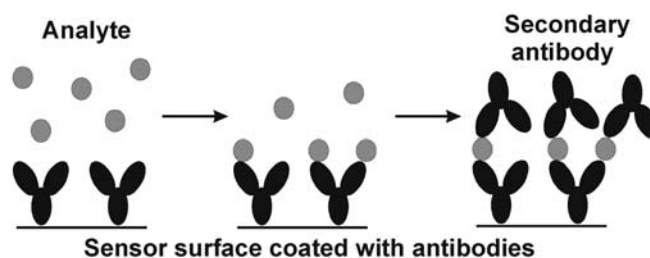


**Fig. 9** Sandwich assay

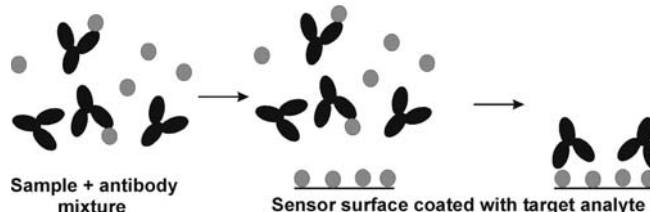


**Fig. 10** Inhibition assay

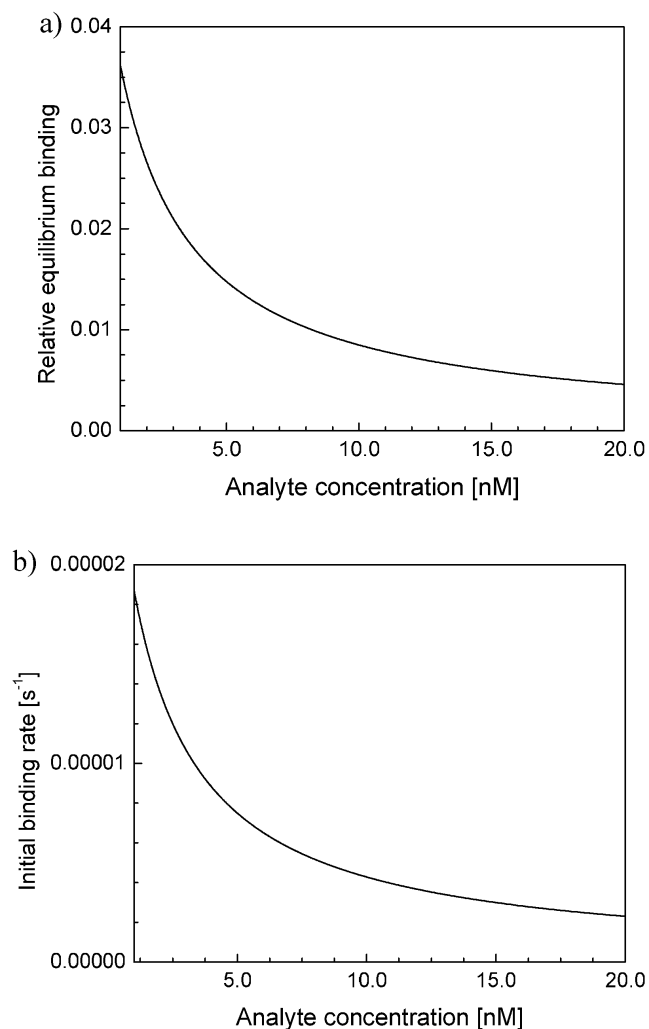


**Fig. 11** Inhibition assay: (a) relative equilibrium binding of the antibody as a function of analyte concentration; (b) initial binding rate as a function of analyte concentration;  $k_a=3\times 10^5 \text{ mol}^{-1} \text{ L s}^{-1}$ ;  $k_d=5\times 10^{-4} \text{ s}^{-1}$ ; antibody concentration  $0.1 \text{ nmol L}^{-1}$

initial binding rate are inversely proportional to analyte concentration, Fig. 11.

### Features and challenges

SPR biosensor technology exhibits various advantageous features. These include in particular:

1. Versatility – generic SPR sensor platforms can be tailored for detection of any analyte, providing a biomolecular recognition element recognizing the analyte is available; analyte does not have to exhibit any special properties such as fluorescence or characteristic absorption and scattering bands.
2. No labels required – binding between the biomolecular recognition element and analyte can be observed directly without the use of radioactive or fluorescent labels.

3. Speed of analysis – the binding event can be observed in real-time providing potentially rapid response.
4. Flexibility – SPR sensors can perform continuous monitoring as well as one-time analyses.

SPR biosensors exhibit two inherent limitations:

1. Specificity of detection – specificity is solely based on the ability of biomolecular recognition elements to recognize and capture analyte. Biomolecular recognition elements may exhibit cross-sensitivity to structurally similar but non-target molecules. If the non-target molecules are present in a sample in a high concentration, sensor response due to the non-target analyte molecules may conceal specific response produced by low levels of target analyte.
2. Sensitivity to interfering effects – similar to other affinity biosensors relying on measurement of refractive index changes, SPR biosensor measurements can be compromised by interfering effects which produce refractive index variations. These include non-specific interaction between the sensor surface and sample (adsorption of non-target molecules by the sensor surface), and background refractive index variations (due to sample temperature and composition fluctuations).

### Advances in SPR biosensor technology

This paper follows up an SPR sensor technology review paper published in *Sensors and Actuators B* in 1999 [9], and therefore focuses primarily on recent advances in SPR biosensor technology. In this section the following areas are discussed in particular: SPR sensor platforms, data analysis, and biomolecular recognition elements.

### Instrumentation

In recent years, research into optical platforms for SPR biosensors has been increasingly application-oriented, targeting specific application areas and providing solutions meeting unique requirements of specific applications. Two important representatives of this trend are: development of laboratory SPR sensor platforms with a large number of sensing channels for high-throughput screening applications and development of mobile SPR sensor platforms for analysis of complex samples in the field.

In traditional multichannel SPR sensors, SPWs were excited via a prism coupler in multiple areas which were arranged perpendicularly to the direction of propagation of SPWs; angular [23] or spectral [24] distribution of reflected light was analyzed to yield information about the measurand in each channel. While this spectroscopic approach led to development of high-performance SPR sensing devices [23], the number of sensing channels which could be realized using this approach was rather limited (<10). In order to increase the number of sensing channels, various SPR sensor platforms have been proposed [25, 26, 27, 28]. One approach is based on SPR imaging

in which a collimated light beam from a polychromatic light source passes through a prism and is made incident on an SPR-active metal layer; the reflected light is detected with a CCD camera after passing through a narrow-band interference filter [25]. This approach has been demonstrated for monitoring of adsorption of a single-stranded DNA-binding protein on to single-stranded DNA patterned into an array of  $500 \times 500$ -micron squares [29]. The choice of operating wavelength for imaging SPR sensors have been discussed by Johansen et al. [30]. An alternative approach [26] is based on detection of spatial changes in the phase of light exciting an SPW and interferometry. Two interferometric schemes have been proposed. In the Mach–Zehnder interferometer-based scheme monochromatic light was split into reference and signal beams; the signal beam passed through a prism and, after reflection from an SPR-active metal layer, was recombined with the reference beam producing an interference pattern on a CCD camera [28]. In the TE–TM polarization interferometer TE and TM polarized beams passed through a prism and, after reflection from an SPR-active surface, were shifted with respect to each other and recombined by means of a polarizer producing an interference pattern on a CCD camera [26]. Another interesting approach is based on SPR microscopy [31] and uses surface scanning and SPWs excited by means of an objective lens [27]. Most recently a new approach has been proposed which is based on spectroscopy of SPW on an array of diffraction gratings [32].

A great deal of research has been focused on development of mobile SPR sensor platforms with referencing capabilities enabling applications of SPR biosensors in out-of-laboratory environments and for analysis of complex samples. The traditional approach consisted in simultaneous SPR measurements in two sensing channels containing different biomolecular recognition element coatings, one with (signal channel) and one without (reference channel) affinity for the analyte, and subtraction of the reference channel response from that of the signal channel [24]. Recently, a new approach to multichannel SPR sensing has been developed which is based on excitation of surface plasmons in different sensing channels at different wavelengths and encoding information from different sensing channels into different regions of the light spectrum. This can be accomplished in a sensing element of special design in which light is made incident on the SPR-active metal at different angles of incidence (Fig. 12a) [33], or by employing a thin dielectric overlayer which shifts the resonant wavelength for a part of the sensing surface to longer wavelengths (Fig. 12b) [34]. This approach has been demonstrated to have capacity to discriminate effects occurring in the proximity of the sensor surface (specific binding, non-specific adsorption) from those occurring in the whole medium (interfering background refractive index fluctuations) which is a prerequisite for advanced referencing [35]. Referencing approaches have been studied [36, 37]. It was found that a residual error for compensation of interfering background refractive index variations is typically 1–3% of the total refractive index change;

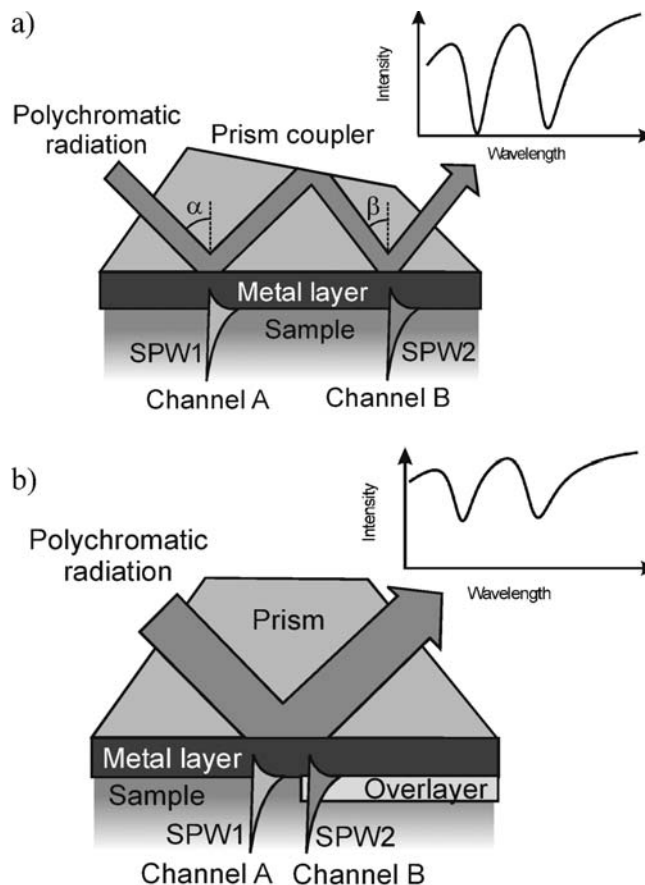
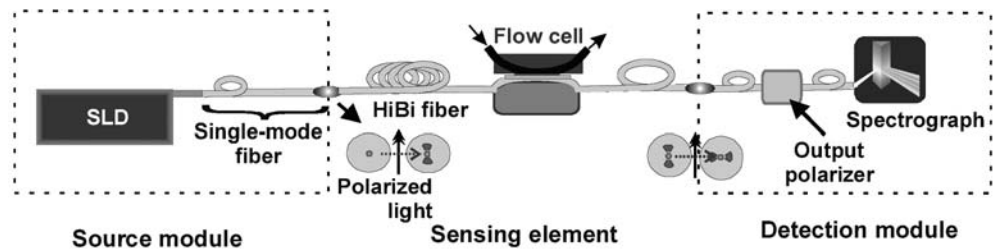


**Fig. 12** Dual-surface-plasmon spectroscopy. (a) Geometry with two different angles of incidence [33]. (b) Geometry with a high refractive index overlayer [34]

compensation for temperature variations is less accurate with an error of 5–10% of the total response due to the temperature change [37].

There is continuing effort to develop miniature SPR platforms based on miniaturized prism couplers [38] and optical fibers. The first fiber optic SPR sensors were based on wavelength-modulation in multimode optical fibers with partly removed cladding and a metal film deposited symmetrically around the exposed section of fiber core [39] or on intensity-modulation in single-mode optical fibers which were side-polished and coated with a thin metal film [40]. These SPR sensors suffered from modal noise (multimode fiber-based sensors) and polarization instability (single-mode fiber-based sensors). Two methods of overcoming the limitation originating from the need to precisely control polarization of light in the single-mode optical fiber-based SPR sensors have been developed. In the first method, light from a polychromatic light source passes through a Lyott fiber optic depolarizer which produces unpolarized light which is then coupled into a fiber optic SPR sensing element. The transmitted light is analyzed with a spectrograph [41]. The second method uses a polarization-maintaining fiber to control polarization of light in the fiber-optic SPR sensing element, Fig. 13. This approach provides best suppression of polarization effects due to fiber

**Fig. 13** SPR sensor based on a polarization-maintaining single-mode optical fiber



deformations resulting in enhanced-stability fiber optic SPR sensors with performance comparable to bulk-optic SPR sensors [42].

Research is also carried out to improve detection capabilities of SPR biosensors by exploiting a special type of an SPW, the so-called long-range surface plasmon. The use of long-range surface plasmons provides two benefits – increased sensitivity and very narrow angular or spectral dips, which makes it possible to determine the spectral position of the SPR dip with a high accuracy [43]. As long-range surface plasma waves penetrate deeper into the probed medium, their use benefits especially biosensors with extended matrices of biomolecular recognition elements [44].

#### Sensor data analysis

Detection limits of SPR biosensors are ultimately constrained by the noise-based precision of the SPR instrument itself. The precision depends on noise contributions made by individual components of an SPR sensor and data processing method. Therefore, study of noise in SPR sensors and development of optimized algorithms for processing data from SPR sensors have received much attention lately. Earlier approaches to understanding the performance of SPR sensor data analysis have included studies of the effects of noise and comparisons between algorithms. Locally-weighted parametric regression and other methods were compared for low- and high-noise detectors, demonstrating that a small number of low-noise detector pixels may outperform a larger but noisier detector array [45]. Linearization of data processing algorithms and an optimal linear data analysis method were proposed as a means of optimizing algorithm parameters [46]. Contribution of analog-to-digital converter resolution and number of pixels in the detector array to the performance of a number of SPR data-analysis algorithms was studied [47]. Also, effects of sensitivity deviations on concentration analyses and kinetic studies have been investigated [48]. Most recently, sources of noise were investigated for a wavelength-modulated SPR sensor. Shot noise of the detector was found to be the dominant source of noise and an analytical formula was derived which allows prediction of the noise of the sensor output based on the detector noise [49].

#### Biomolecular recognition elements and their immobilization

The main types of biomolecular recognition elements used in SPR biosensors include antibodies, nucleic acids and biomimetic materials. Antibodies are used most frequently because of their high affinity, versatility, and commercial availability. Various immobilization chemistries have been developed to attach antibodies to SPR-active gold films. Traditional approaches include formation of streptavidin layer on the gold surface followed by attachment of biotinylated antibodies [50], use of self-assembled alkanethiol films with suitable reactive groups [51], use of a hydrogel matrix composed of carboxyl-methylated dextran chains which can be modified allowing antibodies to be attached via surface-exposed amine, carboxyl, sulfhydryl, and aldehyde groups [52]. Alternatively, SPR sensing surfaces may be functionalized by thin polymer films to which antibodies are coupled via amino groups [53]. Protein contact printing has been examined for spatially-controlled attachment of bovine serum albumin (BSA) and dinitrophenylated BSA onto adjacent reference and signal channels of a dual-channel SPR sensor [54]. DNA can be immobilized on gold SPR sensor surfaces by formation of a streptavidin layer on a gold surface followed by attachment of biotinylated DNA [55]. A multistep surface modification based on alkanethiol self-assembled monolayers has also been used to attach DNA to gold surfaces [56]. Recently, biomimetic materials consisting in molecularly imprinted polymers (MIPs) have been exploited in SPR biosensors [57].

#### Applications of SPR biosensors

Two major application areas for SPR biosensing are in detection and identification of biological analytes and biophysical analysis of biomolecular interactions. This review focuses on applications for detection and identification of biological analytes; recent advances in SPR-based biomolecular interaction analysis can be found in Ref. [58].

Numerous SPR biosensors have been developed for detection and identification of specific analytes. These biosensors use a number of platform designs, biomolecular recognition elements and detection formats. The choice of detection format for a particular application depends on size of target analyte molecules, binding characteristics of biomolecular recognition element, and the range of ana-

lyte concentrations to be measured. Direct detection is usually preferred in applications where direct binding of analyte of concentrations of interest produces a sufficient response. If necessary, the lowest detection limits of the direct SPR biosensors can be improved by using sandwich assay. The secondary antibodies may also be coupled to large particles such as latex particles [59] and gold beads [60] to further enhance the SPR sensor response. Smaller analytes (molecular weight <1000) are usually measured using inhibition assay.

### Detection of small analytes

SPR biosensors have been demonstrated for small analytes relevant to environmental protection (simazine and atrazine), medicine (morphine, methamphetamine, and theophylline), and food safety (fumonisin B1, sulfamethazine, and sulfadiazine). Minunni and Mascini used an

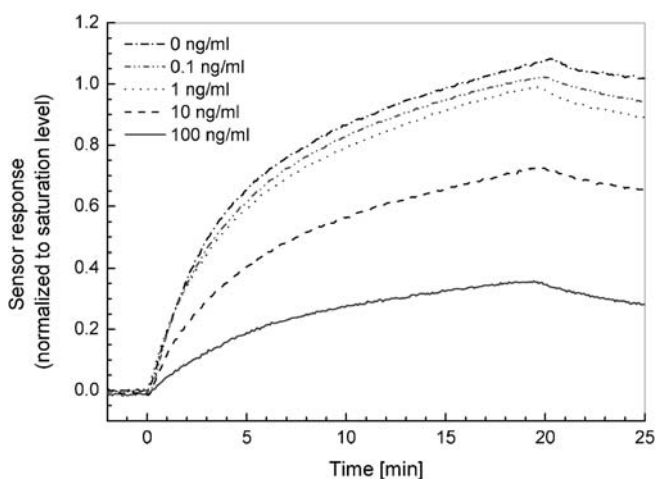


**Fig. 14** Detection of atrazine using inhibition assay. Kinetic response

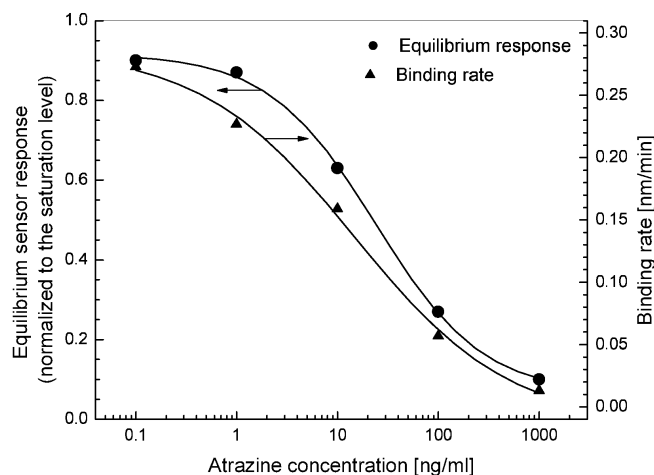


**Fig. 15** Detection of atrazine using inhibition assay. Equilibrium response and initial binding rate as a function of atrazine concentration

SPR sensor and binding inhibition assay to detect atrazine [61]. Monoclonal antibodies against atrazine were mixed with a sample containing atrazine and free antibody concentration was determined by exposing the sample to an atrazine derivative-coated SPR biosensor. A detection limit of  $0.05 \text{ ng mL}^{-1}$  was achieved [61]. Figures 14 and 15 show typical sensorgrams for binding inhibition assay detection of atrazine using a wavelength-modulated SPR sensor; the antibody concentration was  $4 \mu\text{g mL}^{-1}$ .

Detection of the triazine herbicide simazine in water samples was demonstrated using an integrated optical SPR sensor and binding inhibition assay involving anti-simazine IgG antibodies or anti-simazine Fab fragments [62, 63]. The lowest detection limit for simazine was determined to be  $0.16 \text{ ng mL}^{-1}$  for anti-simazine IgG antibodies and  $0.11 \text{ ng mL}^{-1}$  for anti-simazine Fab fragments [63]. Morphine detection based on an SPR sensor and binding inhibition assay was reported by Miura et al. [64], who detected morphine at concentrations down to  $0.1 \text{ ng mL}^{-1}$ . Sakai et al. developed an SPR biosensor for detection of methamphetamine using binding inhibition assay; the lowest detection limit was determined to be  $0.1 \text{ ng mL}^{-1}$  [65]. Direct detection of fumonisin B1 in aqueous samples was demonstrated by Mullet et al. using a laboratory SPR system with angular modulation and polyclonal antibodies [66]. The detection limit was determined to be  $50 \text{ ng mL}^{-1}$ . Sulfamethazine in milk was detected using a commercial SPR system based on angular modulation (Biacore) and binding inhibition assay involving anti-sulfamethazine polyclonal antibodies. The lowest detection limit for sulfamethazine was determined to be  $1 \text{ ng mL}^{-1}$  [67] and  $2 \text{ ng mL}^{-1}$  [68]. Baxter et al. demonstrated SPR biosensor-based detection of streptomycin in milk using a commercial SPR biosensor (Biacore 2000) and inhibition assay involving polyclonal anti-streptomycin antibodies. The lowest detection limit of the SPR biosensor for streptomycin was determined to be  $4 \text{ ng mL}^{-1}$  [69]. Elliott et al. demonstrated detection of sulfadiazine in pig bile using a commercial SPR biosensor (Biacore) and inhibition assay with a detection limit of  $20 \text{ ng mL}^{-1}$  [70]. A laboratory SPR biosensor with angular modulation was combined with a molecularly imprinted polymer for detection of theophylline by Lai et al. For aqueous samples the lowest detection limit was estimated at  $0.4 \text{ mg mL}^{-1}$  [57].

### Detection of medium-size analytes

Examples of medium-size analytes detected by SPR biosensor technology include food safety-related analytes such as staphylococcal enterotoxin B, botulinum toxin, and *E. coli* enterotoxin. Choi et al. demonstrated a direct SPR biosensor for botulinum toxin using a commercial SPR biosensor (Biacore X) and monoclonal antibodies; this biosensor was able to detect botulinum toxin in buffer at a concentration of  $2.5 \mu\text{g mL}^{-1}$  [71]. Spangler et al. demonstrated direct detection of *E. coli* enterotoxin in aqueous solutions; the lowest detection limit was established to be  $6 \mu\text{g mL}^{-1}$  [72]. Detection of staphylococcal

enterotoxin B was performed using a commercial angular sensor (Biacore 3000) [73] and laboratory wavelength modulation-based SPR sensors [74]. The lowest detection limits were 1–10 ng mL<sup>-1</sup> (in milk and meat) [73], 5 ng mL<sup>-1</sup> (direct detection in buffer), and 0.5 ng mL<sup>-1</sup> (sandwich assay in buffer and milk) [74]. A typical sensorgram for detection of Staphylococcal enterotoxins B (SEB) is shown in Fig. 16 [74]. Figure 17a shows the equilibrium sensor response for both the direct capture of SEB and amplifi-

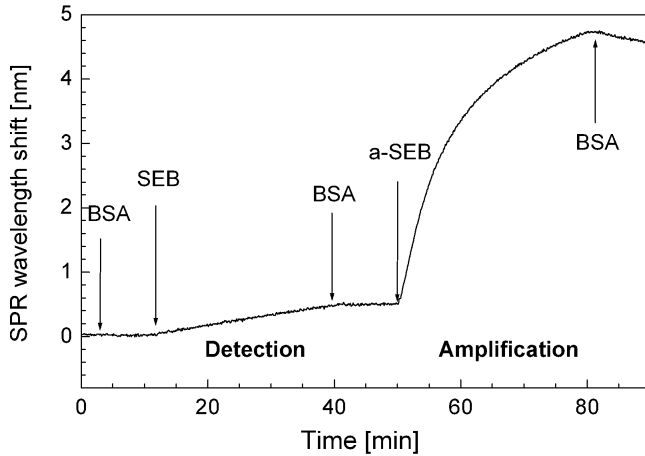


**Fig. 16** Detection of Staphylococcal enterotoxin B using sandwich assay. Kinetic response [74]

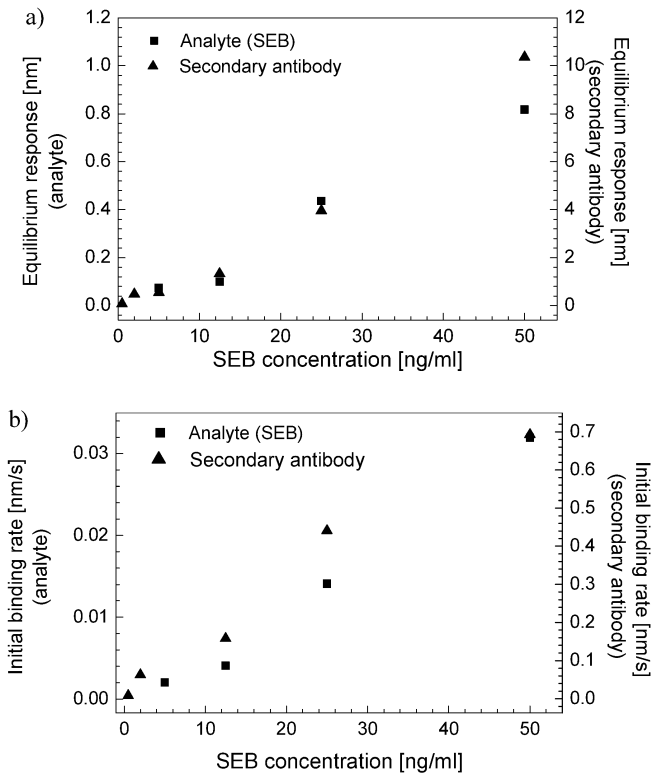


**Fig. 17** Detection of Staphylococcal enterotoxin B. (a) Equilibrium response for different concentrations of SEB. (b) Initial binding rate for different concentrations of SEB [74]

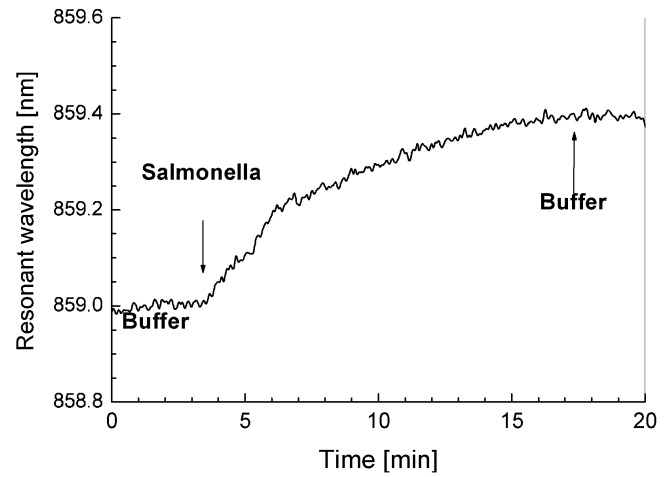


**Fig. 18** Direct detection of *Salmonella enteritidis*. Kinetic response to *Salmonella* at a concentration of 10<sup>6</sup> cfu mL<sup>-1</sup>

cation by secondary antibodies as a function of SEB concentration. The use of secondary antibodies provides 10-fold increase in the sensor response. In Fig. 17b, initial binding rates for SEB and secondary antibody concentration are shown for several SEB concentrations [74].

#### Detection of large analytes

Representatives of large analytes targeted by SPR biosensor technology include bacterial pathogens such as *Escherichia coli*, *Salmonella enteritidis*, and *Listeria monocytogenes*. Detection of *Escherichia coli* O157:H7 was performed by Fratamico et al. who used an angular-modulation commercial SPR sensor and sandwich assay [75]. They used monoclonal antibodies immobilized on the sensor surface for capturing *E. coli* and polyclonal secondary antibodies for enhancing the specific sensor response. The lowest detection limit for *E. coli* was established at 5×10<sup>7</sup> cfu mL<sup>-1</sup>. Direct detection of *Salmonella enteritidis* and *Listeria monocytogenes* at concentrations down to 10<sup>6</sup> cfu mL<sup>-1</sup> was demonstrated by Koubová et al. using a laboratory wavelength-modulated SPR sensor and monoclonal antibodies [76]. A sensorgram illustrating direct detection of *Salmonella enteritidis* is shown in Fig. 18.

The main challenges in detecting bacterial analytes at lower levels include the low concentration of a particular antigen relative to total cellular material and slow diffusion of bacterial cells to sensor surface [77].

#### Commercialization of SPR biosensors

The first commercial SPR biosensor was launched by Biacore International AB in 1990. In the following decade, Biacore has developed a range of laboratory SPR instruments (Biacore 1000, Biacore 2000, Biacore 3000, Biacore C, Biacore X, Biacore J, Biacore Q) [78]. Most recently the Biacore S51 has been developed which offers

higher sensitivity and throughput. Other SPR sensors have been developed by British Windsor Scientific (IBIS) [79], Nippon Laser and Electronics Laboratory (SPR-670 and SPR-CELLIA) [80], Texas Instruments (Spreeta) [81], and Analytical  $\mu$ -Systems (BIO-SUPLAR 2) [82].

## Outlook

Over the past ten years, surface plasmon resonance (SPR) biosensor technology has made great strides, and a large number of SPR sensor platforms, biomolecular recognition elements, and measurement formats have been developed. There has been growing interest in commercialization of SPR biosensor technology leading to a number of systems available on today's market. SPR biosensors have played a significant role in research into biomolecules and their interactions and have been increasingly used for detection and identification of chemical and biological substances. SPR biosensors have been particularly successful for detection of small and medium size analytes, a number of which have been detected at practically relevant levels. Detection limits for large analytes such as bacteria and viruses still need to be improved to meet today's needs.

Undoubtedly, future development of SPR biosensors will be driven by the needs of the consumer. SPR biosensor technology has the potential to benefit numerous important fields including pharmaceutical research, medical diagnostics, environmental monitoring, food safety, and security. Applications in these areas present unique challenges and impose special requirement on analytical technologies. Pharmaceutical research, which was fast to adopt optical biosensors, needs laboratory-based high-throughput systems with high sensitivity to facilitate parallel screening. Medicine would benefit from high-throughput diagnostic tools for centralized laboratories and from compact diagnostic systems dedicated to selected diagnostic applications which could be used at clinics. In addition, there is a growing interest in tools for home medical (self-) diagnostics. Mobile analytical systems enabling rapid detection of food-borne pathogens in food would be important for food producers, processors, distributors and regulatory agencies and thus benefit the food safety. Environmental monitoring would benefit from detection systems which could be deployed in the field for continuous monitoring and from mobile systems enabling fast identification of environmental threat. SPR biosensors could also play an important role in defense, where fast, portable and rugged units are needed for early detection and identification of biological warfare agents in the field. Development of these systems will require significant advances in miniaturization of SPR biosensing platforms, development of robust biomolecular recognition elements with high specificity and long storage life, integration of SPR sensor platforms with microfluidic devices, and application-specific sampling systems.

**Acknowledgement** This work was supported by the Grant Agency of the Czech Republic under contracts 102/03/0633, 303/03/0249, and 203/02/1326.

## References

- Ghindilis AL, Atanasov P, Wilkins M, Wilkins E (1998) *Biosens Bioelectron* 13:113–131
- Chu X, Lin ZH, Shen GL, Yu RQM (1995) *Analyst* 120: 2829–2832
- Gauglitz G (1996) *Opto-chemical and opto-immuno sensors, sensor update, vol 1*. VCH, Weinheim
- Rowe-Taitt CA, Hazzard JW, Hoffman KE, Cras JJ, Golden JP, Ligler FS (2000) *Biosens Bioelectron* 15:579–589
- Piehler J, Brecht A, Gauglitz G (1996) *Anal Chem* 68:139–143
- Heideman RG, Kooyman RPH, Greve J (1993) *Sens Actuators B* 10:209–217
- Clerc D, Lukosz W (1994) *Sens Actuators B* 19:581–586
- Cush R, Cronin JM, Stewart WJ, Maule CH, Molloy J, Goddard NJ (1993) *Biosens Bioelectron* 8:347–353
- Homola J, Yee S, Gauglitz G (1999) *Sens Actuators B* 54:3–15
- Homola J, Yee S, Myszka D (2002) Surface plasmon biosensors. In: Ligler FS, Taitt CR (eds) *Optical biosensors: present and future*. Elsevier
- Rabbany SY, Lane WJ, Marganski WA, Kusterbeck AW, Ligler FS (2000) *J Immunol Methods* 246:69–77
- Boardman AD (1982) (ed) *Electromagnetic surface modes*. Wiley, Chichester
- Reather H (1983) *Surface plasmons on smooth and rough surfaces and on gratings*, Springer tracts in modern physics, vol 111. Springer, Berlin Heidelberg New York
- Snyder AW, Love JD (1983) *Optical waveguide theory*. Chapman and Hall, London
- Parriaux O, Voirin G (1990) *Sens Actuators A* 21–23:1137
- Hutley MC (1982) *Diffraction gratings*. Academic Press, London
- Kooyman RPH, Kolkman H, van Gent J, Greve J (1988) *Anal Chim Acta* 213:35–45
- Yeaman EM (1996) *Biosens Bioelectron* 11:635–649
- Homola J (1997) *Sens Actuators B* 41:207–211
- Homola J, Koudela I, Yee S (1999) *Sens Actuators B* 54:16–24
- Edwards PR, Leatherbarrow RJ (1997) *Anal Biochem* 246:1–6
- Vijayendran RA, Ligler FS, Leckband DE (1999) *Anal Chem* 71:5405–5412
- Löfås S, Malmqvist M, Rönnerberg I, Stenberg E, Liedberg B, Lundström I (1991) *Sens Actuators B* 5:79
- Nenninger GG, Clendenning JB, Furlong CE, Yee S (1998) *Sens Actuators B* 51:38
- Jordan CE, Frutos AG, Thiel AJ, Corn RM (1997) *Anal Chem* 69:4939
- Nikitin PI, Beloglazov AA, Kabashin AV, Valeiko MV, Kochergin V E (1999) *Sens Actuators B* 54:43
- Kano H, Knoll W (2000) *Optics Communications* 182:11–15
- Kabashin A V, Nikitin P I (1998) *Opt Commun* 150:5–8
- Nelson BP, Frutos AG, Brockman JM, Corn RM (1999) *Anal Chem* 71:3928–3934
- Johansen K, Arwin H, Lundström I, Liedberg B (2000) *Rev Sci Instrum* 71:3530–3538
- Rothenhäusler B, Knoll W (1988) *Nature* 332:688
- Dostálek J, Homola J, Miler M (2002) *EUROPT(R)ODE VI*, Manchester, UK, Book of Abstracts, 265
- Homola J, Dostálek J, Čtyroký J (2001) *Proc SPIE* 4416:86
- Homola J, Lu HB, Yee S (1999) *Electr Lett* 35:1105
- Homola J, Lu HB, Nenninger GG, Dostálek J, Yee S (2001) *Sens Actuators B* 76:403–410
- Ober RJ, Ward E S (1999) *Anal Biochem* 271:70–80
- Homola J, Dostálek J, Piliarik M, Yee S (2002) *EUROPT(R)ODE VI*, Manchester, UK, Book of Abstracts, 71
- Stemmler I, Brecht A, Gauglitz G (1999) *Sens Actuators B* 54:98–105
- Jorgenson RC, Yee S (1993) *Sens Actuators B* 12:213
- Homola J (1995) *Sens Actuators B* 29:401–405
- Homola J, Piliarik M, Slavík R, Čtyroký J (2001) *SPIE Proc* 4416:82–85
- Piliarik M, Homola J, Maníková Z, Čtyroký J (2003) *Sens Actuators B* 90:236–242

43. Nenninger GG, Tobiška P, Homola J, Yee S (2001) *Sens Actuators B* 74:145
44. Liedberg B, Lundström I, Stenberg E (1993) *Sens Actuators B* 11:63
45. Johnston KS, Booksh KS, Chinowsky TM, Yee S (1999) *Sens Actuators B* 54:80–88
46. Chinowsky TM, Jung LS, Yee S (1999) *Sens Actuators B* 54:89–97
47. Johansen K, Ståhlberg R, Lunström I, Liedberg B (2000) *Meas Sci Technol* 11:1630–1638
48. Johansen K, Lundström I, Liedberg B (2000) *Biosens Bioelectron* 15:503–509
49. Nenninger GG, Piliarik M, Homola J (2002) *Meas Sci Technol* 13:2038–2046
50. Morgan H, Taylor DM, (1992) *Biosens Bioelectron* 7:405–410
51. Duschl C, Sevin-Landais A, Vogel H (1995) *Biophys J* 70:1985
52. Löfås S, Malmqvist M, Rönnerberg I, Stenberg E, Liedberg B, Lundström I (1991) *Sens Actuators B* 5:79
53. Nakamura R, Muguruma H, Ikebukuro K, Sasaki S, Nagata R, Karube I, Pedersen H (1997) *Anal Chem* 69:4649
54. Lu HB, Homola J, Campbell CT, Nenninger GG, Yee S, Ratner BD (2001) *Sens Actuators B* 74:91–99
55. Watts HJ, Yeung D, Parkes H (1995) *Anal Chem* 67:4283–4289
56. Brockman JM, Frutos AG, Corn RM (1999) *J Am Chem Soc* 121:8044–8051
57. Lai EPC, Fafara A, VanderNoot VA, Kono M, Polsky B (1998) *Can J Chem* 76:265–273
58. Rich RL, Myszka DG (2002) *J Mol Recognit* 15:352–376
59. Severs AH, Schasfoort RBM (1993) *Biosens Bioelectron* 8:365
60. Leung PT, Pollard-Knight D, Malan GP, Finlan MF (1994) *Sens Actuators B* 22:175
61. Minunni M, Mascini M (1993) *Anal Lett* 26:1441
62. Mouvet C, Harris RD, Maciag C, Luff BJ, Wilkinson JS, Piehler J, Brecht A, Gauglitz G, Abuknesha R, Ismail G (1997) *Anal Chim Acta* 338:109
63. Harris RD, Luff BJ, Wilkinson JS, Piehler J, Brecht A, Gauglitz G, Abuknesha RA (1999) *Biosens Bioelectron* 14:377
64. Miura N, Ogata K, Sakai G, Uda T, Yamazoe N (1997) *Chem Lett* 8:713
65. Sakai G, Nakata S, Uda T, Miura N, Yamazoe N (1999) *Electrochim Acta* 44:3849
66. Mullett W, Edward PC, Yeung MJ (1998) *Anal Biochem* 258:161–167
67. Sternesjo A, Mellgren C, Björck L (1996) *ACS Symp Ser* 621:463–470
68. Gaudin V, Pavy M-L (1999) *JAOAC Int* 82:1316–1320
69. Baxter GA, Ferguson JP, O’Conner MC, Elliott CT (2001) *J Agric Food Chem* 49:3204–3207
70. Elliot CT, Baxter GA, Crooks SRH, McCaughey WJ (1999) *Food Agric Immunol* 11:19–28
71. Choi K, Seo W, Cha S, Choi J (1998) *J Biochem Mol Biol* 31:101–105
72. Spangler BD, Wilkinson EA, Murphy JT, Tyler BJ (2001) *Anal Chim Acta* 444:149–161
73. Rasooly A (2001) *J Food Prot* 64:37–43
74. Homola J, Dostálek J, Chen S, Rasooly A, Jiang S, Yee S (2002) *Int J Food Microbiol* 75:61–69
75. Fratamico PM, Strobaugh TP, Medina MB, Gehring AG (1998) *Biotechnol Tech* 12:571–576
76. Koubová V, Brynda E, Karasová L, Škvor J, Homola J, Dostálek J, Tobiška P, Rošický J (2001) *Sens Actuators B* 74:100–105
77. Perkins EA, Squirrel DJ (2000) *Biosens Bioelectron* 14:853
78. Biacore website [www.biacore.com](http://www.biacore.com)
79. IBIS Technologies website [www.ibis-spr.nl](http://www.ibis-spr.nl)
80. Nippon Laser and Electronics Laboratory website [www.nle-lab.co.jp/English/ZO-HOME.htm](http://www.nle-lab.co.jp/English/ZO-HOME.htm)
81. Texas Instruments website [www.ti.com/sc/docs/products/msp/control/spreet](http://www.ti.com/sc/docs/products/msp/control/spreet)
82. Analytical  $\mu$ -Systems website [www.micro-systems.de](http://www.micro-systems.de)